



LAWRENCE
LIVERMORE
NATIONAL
LABORATORY

STOCHASTIC JOINT INVERSION OF A GEOHERMAL PROSPECT

R. J. Mellors, A. Ramirez, A. Tompson, M. Chen, X.
Yang, K. Dyer, J. Wagoner, W. Foxall, W.
Trainor-Guitton

January 30, 2013

Stanford Geothermal Workshop
Palo Alto, CA, United States
February 11, 2013 through February 13, 2013

Disclaimer

This document was prepared as an account of work sponsored by an agency of the United States government. Neither the United States government nor Lawrence Livermore National Security, LLC, nor any of their employees makes any warranty, expressed or implied, or assumes any legal liability or responsibility for the accuracy, completeness, or usefulness of any information, apparatus, product, or process disclosed, or represents that its use would not infringe privately owned rights. Reference herein to any specific commercial product, process, or service by trade name, trademark, manufacturer, or otherwise does not necessarily constitute or imply its endorsement, recommendation, or favoring by the United States government or Lawrence Livermore National Security, LLC. The views and opinions of authors expressed herein do not necessarily state or reflect those of the United States government or Lawrence Livermore National Security, LLC, and shall not be used for advertising or product endorsement purposes.

STOCHASTIC JOINT INVERSION OF A GEOTHERMAL PROSPECT

R. J. Mellors, A. Ramirez, A. Tompson, M. Chen, X. Yang, K. Dyer, J. Wagoner, W. Foxall, and W. Trainor-Guitton

Lawrence Livermore National Laboratory
7000 East Avenue
Livermore, CA, 94550, USA
e-mail: mellors1@llnl.gov

ABSTRACT

We are developing a stochastic inverse algorithm to jointly analyze multiple geophysical and hydrological datasets for a geothermal prospect. The purpose is to improve prospect evaluation and estimate the likelihood of useful temperature and fluid flow fields at depth. We combine Bayesian inference with a Markov Chain Monte Carlo (MCMC) global search to conduct a staged inversion of the different data sets. The results consist of a detailed description of the uncertainty in the solution as well as a suite of alternative geothermal reservoir models. The method is highly flexible and capable of accommodating multiple and diverse datasets.

INTRODUCTION

The primary objective of geothermal exploration is to find and characterize a commercial source of geothermal energy. Favorable geothermal prospects require three main elements: heat, water, and hydraulic permeability. As all three elements are difficult to resolve in the subsurface, geothermal exploration usually employs multiple geophysical, geological, hydrological, and geochemical methods to capture the most complete characterization of a geothermal system possible. Ideally, a complete model will include contributions from, and, in the end, be consistent with all data sources.

A principal goal in characterizing a geothermal prospect is to produce a quantitative predictive capability to describe the temperature and fluid flow distributions in the subsurface prior to any significant drilling. This paper outlines a joint inversion methodology to utilize multiple geophysical, thermal,

and hydrological data sets in the construction of such a model. Recognizing the inherent uncertainties in structural, parametric, and other characteristics of subsurface systems, the approach uses stochastic representations of important variables or structural features within a generalized Markov Chain Monte Carlo (MCMC) inversion process. Success in implementing joint inversion with geophysics and hydrology may allow inclusion of geochemical or tracer studies in the future. In some ways, it is similar to the approach taken by Jardani and Revil (2009).

The MCMC inversion process will yield a suite of plausible results rather than one single answer. This algorithm possesses several advantages: it is flexible, searches the global solution space defined by the stochastic variable distributions, and provides robust uncertainty estimates. The results are expressed as a range of models along with an associated probability density function. This aids in providing a quantitative evaluation of the prospect.

This paper describes our approach and initial results from our implementation to a simplified example problem, both of which are still in development. Our current focus is to evaluate algorithm performance and parametric sensitivities. A significant question is whether this type of inversion, which requires thousands of runs, is feasible for reasonably complex models. The example problem is based on a prospect located in the western Salton trough in California, adjacent to Superstition Mountain, (Figure 1) and currently under investigation by the Navy geothermal program (e.g. Bjornstad et al., 2006; Tiedeman et al., 2011) We chose this site largely because geological and geophysical data were readily available.

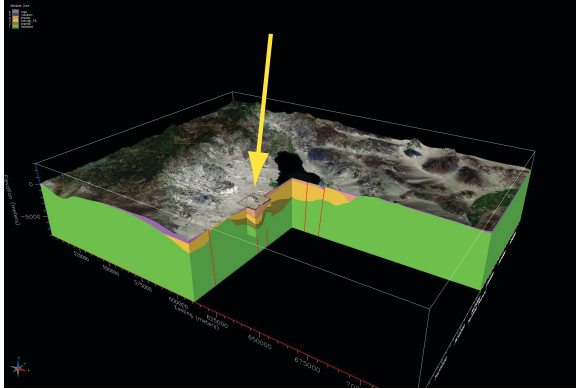


Figure 1: Perspective view (to NW) of region showing the Salton Sea in center. Green is basement and the other colors represent sedimentary or volcanics. Red lines are faults. Arrow marks prospect.

Within the example problem, we are seeking to match vertical temperature profiles observed in a set of three exploration “NAFEC” wells (Figure 2) while simultaneously reproduce measured electrical resistivity distribution. An initial 3-D geologic model defining structural geometry is used as a starting basis for the model. Uncertain material properties such as permeability, porosity, and heat capacity are allowed to vary in the simulation process, as well as certain structural characteristics such as the extent and properties of a perceived fault zone. The simulation algorithm begins by posing *a priori* statistical distributions for these uncertain properties and structural characteristics. A staged MCMC approach is then initiated, first to develop a space of plausible solutions drawn from these distributions and, second, to narrow the space to a subset that is found consistent with temperature and resistivity data.

Specifically, in the first stage of the MCMC process (Figure 3), a 3-D hydrothermal flow model is used to predict equilibrium (steady state) temperature and fluid flow fields for specific model configurations drawn from the uncertain parameter distributions, which are then compared to the measured temperature profiles. Next, in the second stage, electrical resistivity distributions from the better matched of these configurations are calculated using output from the first stage and compared to the resistivity observations. Results are presented as a ranked set of all sampled models along with inferred probability distributions. Additional geophysical constraints such as gravity or magneto-telluric observations will be added in the future.

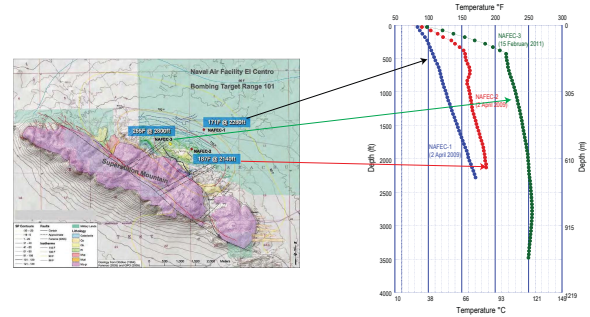


Figure 2: Geologic map of prospect showing surface geology and geophysical measurements with temperature profiles of the three test wells. From Tiedeman et al., 2011. Thermal profiles of the three wells.

METHOD

Our inversion algorithm applies Bayesian inference implemented with an efficient Monte Carlo-Markov Chain (MCMC) global search approach to carry out a staged inversion of the different data sets, based on the method proposed by Mosegaard and Tarantola, (1995). This stochastic inversion selects alternative models that are consistent with available data and ranks them according to the probability that the models represent reality. Joint inversion is accomplished by cascading computational stages, one for each data set. In order for a particular geologic and hydrothermal model to be included in the posterior distribution, it must be accepted by all of the stages. Therefore, the models in the posterior distribution are consistent with all of the data. The procedure is guaranteed to converge to this unique, invariant limiting distribution from any starting trial model, provided that there are sufficient steps (trials) in the Markov chain.

The basic MCMC procedure for this problem is illustrated in Figure 3. An initial geologic model that includes a hydrothermal system is created and a set of initial model parameters is proposed. In our test case, the basic geologic model was based on analyses of previous work near Superstition Mountain (e.g., Dutcher et al., 1972; Loeltz, et al., 1975; Bjornstad et al., 2006; Tiedeman et al., 2011; Tompson et al, 2008). The initial hydrologic model parameters include permeability and boundary pressures and temperatures. For each set of proposed parameters, the desired variables (in this case, temperature profiles at three exploration wells) are calculated and compared to the observed data during the inversion.

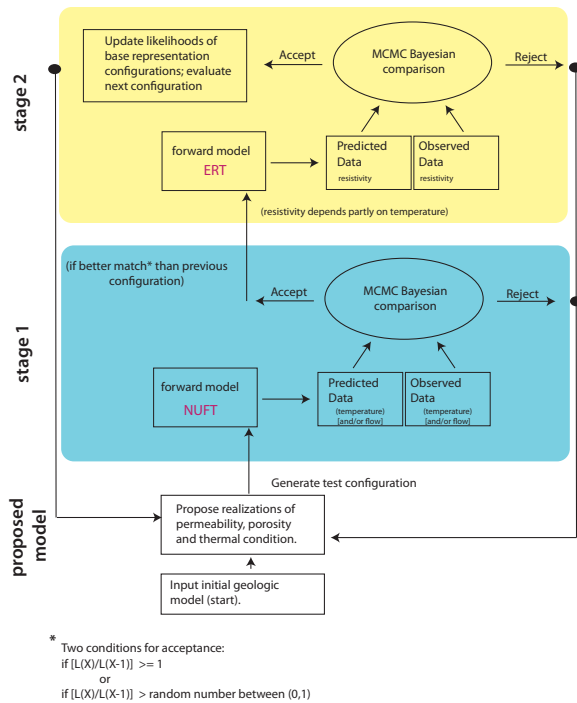


Figure 3: Schematic diagram of the two-stage inversion method. An initial geologic model with hydrologic and thermal constraints is selected. In stage one, it is run until equilibrium using NUFT and temperature is compared with observations. In stage two, assuming stage one acceptance, the expected resistivity of the model is calculated and then compared with the data. The final output is a ranked set of models and associated probabilities.

The likelihood that the proposed model reproduces the true geothermal system properties is calculated from the fit of the calculated data to the actual observations, assuming an estimate of the data error. If the likelihood is acceptable, then that geologic model is included in the posterior distribution, and a new trial model is proposed. The decision to accept/reject is probabilistic (Metropolis et. al., 1953). The proposed mode is always accepted when its likelihood ($L(x+1)$) is better than the that of the previous model ($L(x)$). Alternatively, when $L(x+1) < L(x)$, the probability of acceptance is $L(x+1)/L(x)$. The second condition is included to allow the search to avoid local minima. Otherwise the model is rejected and the process is repeated with a new proposal. This cycle is repeated until the posterior distribution converges to a stable solution, which typically requires thousands of iterations.

In the sequence of Monte Carlo replicates, each new simulation is drawn from statistical distributions of the uncertain parameters or variables. For example,

the permeability is defined by individual log normal distributions in each geologic unit and is correlated with porosity. The bulk thermal conductivity of the formation as a whole is controlled by the intrinsic thermal conductivities of the rock and water and by the saturated porosity. The bulk electrical resistivity of the formation is a function of its temperature and the intrinsic resistivity of rock and groundwater, the latter of which is heavily influenced by its salinity. Although fluid resistivity is held fixed in the present implementation, it may become a powerful constraint in future steps owing to significant salinity contrasts in the basin groundwater (Tompson et al., 2008).

The stochastic inversion framework is written in Python and incorporates various compiled forward codes for each modeled step of the process. We have adapted hydrothermal fluid flow and DC resistivity models into the current version of the framework and will add others as the project matures. Fluid and heat flow are simulated using NUFT (Nonisothermal, Unsaturated Flow and Transport), a 3-D multi-phase hydrothermal flow and transport model based upon an integrated finite difference discretization (Nitao, 1998, 2000). Electrical resistivity is simulated using Multibh, a 3-D finite difference forward modeling code that predicts electrical resistance for arbitrary electrode configurations and electrical resistivity models (LaBrecque et al., 1999). We recognize that DC resistivity is not commonly used in geothermal exploration but the code was available and we are essentially using it as a placeholder in the inversion framework for a magnetotelluric (MT) code whose development is in progress.

The flexibility of the algorithm makes adding additional models or codes straightforward, although use of different grid or meshing schemes in the underlying suite of models can add complications.

PROVISIONAL MODEL & INITIAL RESULTS

Figure 4 shows an initial bounded domain that has been used for the preliminary applications of the hydrothermal flow and electrical resistivity models. The domain is parallel with the NW/SW orientation of Superstition Mountain and primary Superstition Mountain fault directions and has been made to extend approximately 6.5 km to the northeast and to a depth of 3.2 km.. The 1.5 km width was chosen to accommodate the earliest calibration and inversion testing exercises and will be expanded later to support larger areas.

The domain has been chosen to incorporate the three “NAFEC” wells that were drilled to depths between 600 and 1000 m (~2000 to 3500 ft). NAFEC-3 lies

close to the mountain in a zone of perceived, cross-oriented faulting. NAFEC-1 lies furthest from the mountain, away from any perceived faulting, while NAFEC-2 lies in between, in both respects. Geophysical, lithological, and temperature logs were obtained in each borehole (e.g., Figure 5), although no water level or water sampling data were taken. The temperature profiles obtained in each well (Figure 2) differed significantly, suggesting geothermal circulation underlying a shallow zone of conduction-only heat flow in NAFEC-3, conduction-only heat flow in NAFEC-1, and a mixture of the two scenarios in NAFEC-2. Maximum measured temperatures in the wells ranged from 77° to 121°C (171° to 250°F).

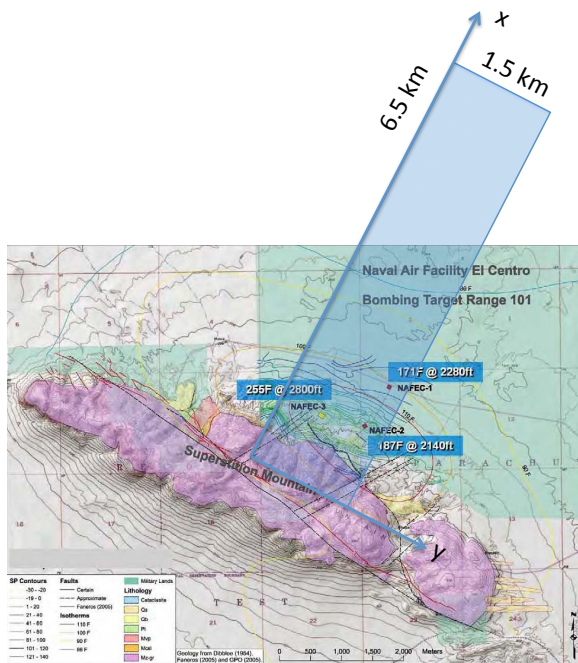


Figure 4: Areal projection of the bounded modeling domain used in the application of the hydrothermal flow and resistivity models.

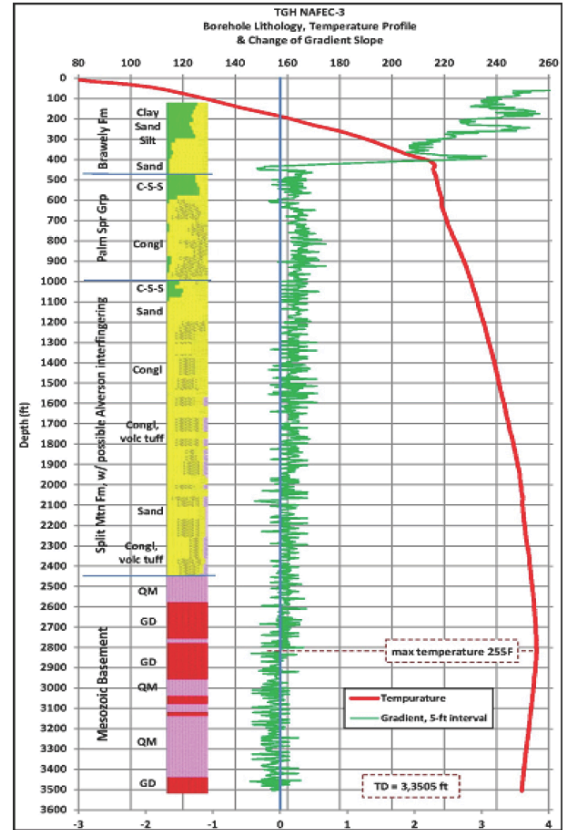


Figure 5: Lithology and thermal log of NAFEC-3 well. Profile suggests a shallow (< 400 ft; 120 m) conduction profile overlying buoyancy drive flow at depth and consistent with water table depth.

Hydrogeologic Conceptualization

A structural and lithologic conceptual model was constructed based on available data (Figures 1, 2, 5). The faults and features shown in Figures 1 and 4, along with observations of temperature profiles in the three wells and hydrothermally altered rock near the surface, have led to a hypothesis of fault-facilitated flow at depth. The preliminary model domain (Figure 6) has adopted several simplifying assumptions in terms of the representation of the geologic model and the physical processes considered. These include:

- An approximate representation of the faulted (granitic) basement and Imperial (sandstone), Borrego / Palm Springs (sandstone and delta sediments), Brawley (sandy sediments) and Post Brawley (lacustrine sediments and clay) formations across the model cross section;
- Two 100-m thick planar faulted zones, one (A) occupying the entire SW face of the domain at $x = 0$, consistent with the Superstition Mountain Faults, and another (B) a hypothesized vertical

fault, perpendicular to and extending away from (A) to the NE, of uncertain length and height, that potentially facilitates hydrothermal flow from depth;

- Specification of a slight downward slope of the top of the model from the SW to the NE, consistent with the local topography;
- Specification of saturated conditions throughout the entire model depth (for now), which will be adjusted later to reflect an apparent water table at a depth between 100 and 120 m (~350 and 400 ft; Dutcher et al., 1972);
- Specification of fixed temperatures of 27° and 150°C at the top and bottom of the domain (~80° and 300°F respectively); and
- Specification of hydrostatic pressures at the SW and NE ends of the model, leading to a slight, imposed hydraulic gradient to the NE.

Within this conceptualization, zones of higher permeability occur within certain layers (Fig. 6, light blue) – the more sandy sediments, for example – and within the faults (Fig 6). The geometry of the hypothesized fault (B) is based on other conjugate faults in the immediate region, such as the Superstition Hill/Elmore Ranch faults a few km to the east. The conceptual model around Superstition Mountain is being refined and locally improved from an earlier model of the Salton Trough (Tompson et al., 2008) constructed using the Earthvision modeling platform (www.dgi.com/).

Grid Generation

Mesh design is a challenge for several reasons. First, there are the customary balances between minimizing computational effort while maintaining adequate spatial resolution, particularly within an MCMC simulation framework. Second, different models in the MCMC framework need to share data, yet may have different meshing requirements. For example, although the hydrothermal flow and resistivity models share the same core mesh (100-m cubic grid, Fig 6), the resistivity mesh must have an extended portion reaching into the far field for boundary condition specification, making it much larger than than the hydrothermal flow model domain.

Within the core modeling mesh (Figure 6), both the hydrothermal flow and resistivity models share the same 100-m cubic grid. Each grid cell is assigned to a particular formation material or unit (such as granite) to which model-related properties (e.g., permeability, porosity, and heat capacity) are assigned. For some units, material properties are drawn from a prior probability distribution during each replicate simulation in the MCMC process; for others, they are held fixed across all MCMC replicates. Note that

changes in the uncertain geometry of the (B) fault are accommodated by re-assigning material “fault” properties for the set of cells that comprise the fault geometry drawn in each replicate.

At the start of the inversion, an initial (replicate 1) model is defined by assigning material properties and the (B) fault geometry from the prescribed statistical distributions. The hydrothermal flow model is then used to calculate a steady state (equilibrium) temperature and flow field under fixed temperature and pressure boundary conditions described above (Figure 7). Computed temperature solutions along the “NAFEC” well locations are then compared against the measured values using a likelihood test (see above). If the flow model is “accepted,” then the resistivity model is run subsequently and its results are similarly compared against the measured resistivity profile. If the flow model is “rejected,” then the resistivity model is not run and a new (replicate 2) flow model is initiated by resampling the parameters from the basic distributions. Results from all accepted models are saved.

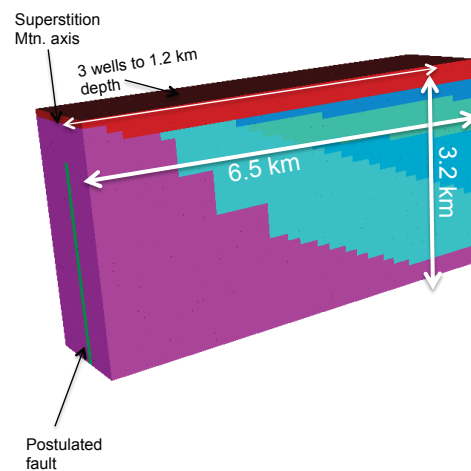


Figure 6: Diagram showing 3D model. Colored units show geological formations and features (e.g. fractured fault zone).

Typically, thousand of replicate runs are required in this process in order to obtain a reasonable set of models that can be “accepted” from both the flow and resistivity perspective, posing a significant computational challenge. In the current example, approximately 16 hours of CPU time on 10 processors were utilized to run four different Markov chains simultaneously. A main constraint in this process is the NUFT model because of its limited parallelization. The results in Figure 7 show that the hypothetical (B) fault can provide a circulation pathway for deeper fluids to migrate into the

shallower formation materials and influence the temperatures observed in the “NAFEC” wells.

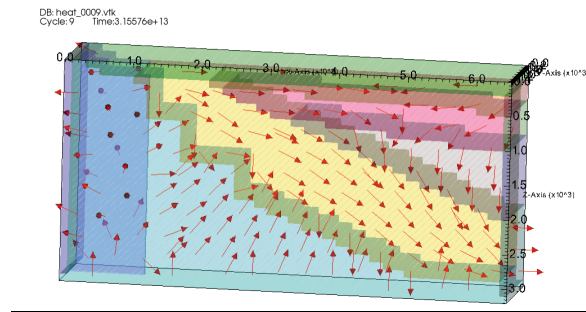


Figure 7: NUFT predicts the temperature, pressure and flow fields for a given realization. The figure shows the simulated groundwater flow lines for a realization where a fault (dark blue) cuts across the granite unit (light blue).

Inversion tests

As an initial test of the inversion code, we constructed a synthetic (control) dataset by forward modeling on a random realization of the prospect model. Figures 8-10 show tests conducted on two subsequent realizations of the prospect, different from the control case. In one representation the fault is contained entirely within the granite and in the other the fault extends into the sediments. Temperature and resistivity data were calculated for both models at the location of the wells (Figure 8). These synthetic datasets were then inverted to test the inversion algorithm and determine if it resolved the original models. Figure 9 shows the top 10% of the inversion results (mean values), with both the recovered temperature distribution and the possible fault geometries, which are displayed as “blurred”. Note that the fault encased completely in granite is poorly constrained relative to the fault, which contacts the sediments. This illustrates the power of the technique to demonstrate the range of possible models. Comparisons of predicted and “observed” data for the nearest of the three wells (marked as red) suggesting acceptable inversion behavior on a simulated dataset are shown in Figure 10.

Additional MCMC simulations based upon inverting the actual observed “NAFEC” data are underway using the same model. Initial results suggest that the profiles are highly sensitive to the location of the hypothetical (B) fault that facilitates the upward geothermal circulation..

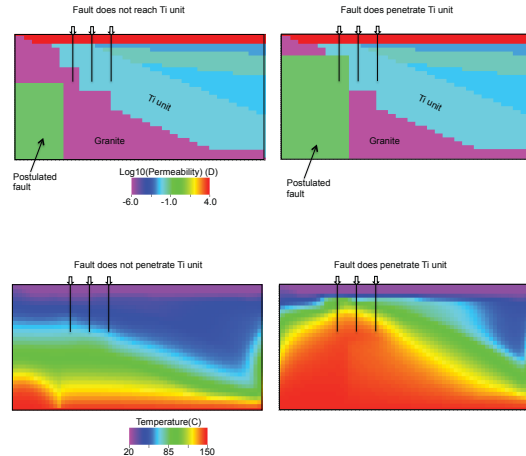


Figure 8: (top) Example showing two synthetic models used to test the inversion based on the Superstition Mountain prospect. Images represent a east-west 2D slice through a 3D model. The left panel shows a fault that is fully contained in the granitic basement. The right panel shows a fault that extends from the granite to the permeable Ti unit (sediment). Colored units show geological formations and features (e.g. fractured fault zone). (bottom) Calculated temperature data for the two models after allowing the hydrothermal model to reach equilibrium. Boundary conditions are fixed. Resistivity is calculated from the temperature, water salinity, and lithology.

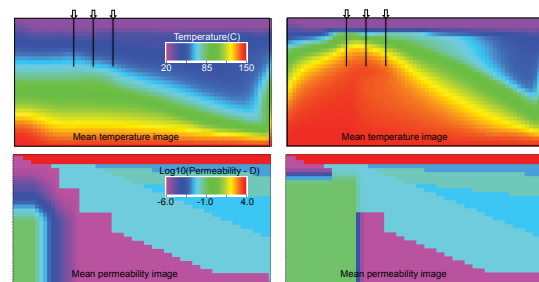


Figure 9: Calculated mean temperature (top) and permeability models (bottom) using top 10% of models with best data fits. Note that the fault appears ‘fuzzy’ in the results. This reflects the range of possible boundaries in the top 10% of the models. This inversion used temperature data only; the combined inversion with resistivity is in progress.

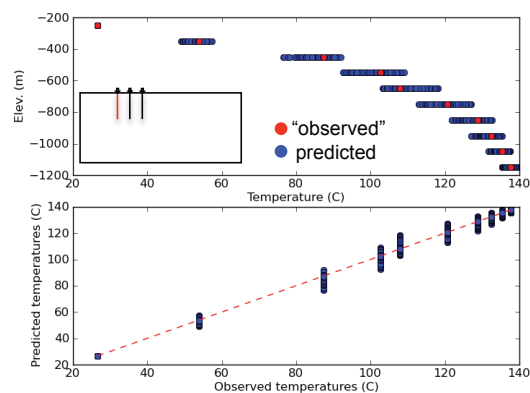


Figure 10: Comparisons of predicted (top 10 % of models) and “observed” data for the nearest of the three wells (marked as red) suggesting acceptable inversion behavior on a simulated dataset

CONCLUSIONS AND NEXT STEPS

We have developed an initial version of the inversion algorithm and software that works well with synthetic data sets. The inversion recovered models that were similar to the true synthetic models and yielded error estimates. The required computational time, while significant, is not impractical. We are currently working on analyzing real temperature data using a similar model.

In the future, we plan to integrate additional geophysical data such as magnetotellurics (MT) and gravity. The flexibility of the approach allows the potential inclusion of other data types such as geochemical signatures and geostatistical-based models of geologic structure. While this will increase computational time, we are investigating the use of reduced-order forward models to reduce computational effort.

We envision the potential use of the algorithm as a method to generate alternative models and corresponding likelihoods to estimate uncertainties associated with a prospect. The initial mesh and model generation is developed to be compatible with commercially available geological modeling packages.

Acknowledgements

This work was performed under the auspices of the U.S. Department of Energy by Lawrence Livermore National Laboratory under Contract DE-AC52-07NA27344.

REFERENCES

- Bjornstad, S.C., Hall B., Unruh J., Richards-Dinger K., (2006), “Geothermal Resource Exploration, NAF El Centro – Superstition Mountain Area, Imperial Valley, California”, GRC 2006.
- Dutcher, L. C., W. F. Hardt, and W. R. Moyle, Jr., (1972): Preliminary appraisal of ground water storage with reference to geothermal resources in the Imperial Valley area, California, Geological Survey Circular 649, prepared in cooperation with the US Bureau of Reclamation, US Geological Survey, Washington, DC.
- Jardani, A., and A. Revil, 2009, Stochastic joint inversion of temperature and self-potential data, *Geophys. Jour. Int.*, 179(1), 640-654.
- LaBrecque, D. J., G. Morelli, W. Daily, A. Ramirez, and P. Lundegard, 1999, Occam's inversion of 3D electrical resistivity, in *Three-Dimensional Electromagnetics*, eds. M. Oristaglio, B Spies, and M. Cooper, pp 575-590, Soc. Expl. Geophys., Tulsa, OK.
- Loeltz, O. J., B. Irelan, J. H. Robison, and F. H. Olmsted (1975), Geohydrologic reconnaissance of the Imperial Valley, California, Geological Survey Professional paper 486 K, US Geological Survey, Washington, DC.
- Metropolis, N., A. Rosenbluth, M. Rosenbluth, A. Teller, and E. Teller (1953), Equation of state calculations by fast computing machines, *J. Chem. Phys.*, 1, no. 6, 1087-1092.
- Mosegaard, K., and A. Tarantola (1995), Monte Carlo sampling of solutions to inverse problems, *Journal of Geophysical Research*, 100, no. B7, 12431-12447.
- Nitao, J.J., User's Manual for the USNT Module of the NUFT Code, Version 3.0 (NP-phase, NC-component, Thermal). Lawrence Livermore National Laboratory, UCRL-MA-130653-Rev-2 (June 1, 2000)
- Nitao, J.J. Nitao, (1998), “Reference manual for the NUFT flow and transport code, Version 2.0”, Technical Report UCRL-MA-130651, Lawrence Livermore National Laboratory, Livermore, CA.
- Ramirez, A., W. McNab, Y. Hao, D. White, J. Johnson, 2011, Final Report: Improved Site Characterization And Storage Prediction Through Stochastic Inversion Of Time-Lapse Geophysical And Geochemical Data, LLNL-TR-480694, Lawrence Livermore National Laboratory, Livermore CA.

- Ramirez, A. L., J.J. Nitao, W.G. Hanley, R.D. Aines, R.E. Glaser, S.K. Sengupta, K.M. Dyer, T.L. Hickling, W.D. Daily, 2005, Stochastic Inversion of Electrical Resistivity Changes Using a Markov Chain, Monte Carlo Approach, Journal of Geophysical Research, vol 110, B02101, doi:10.1029/2004JB003449, also in UCRL-JRNL-155048 Rev. 3, Lawrence Livermore National Lab., Livermore CA.
- Tiedeman, A., S. Bjornstad, S. Alm, L. Frazier, D. Meade, C. Page, M. Lazaro, J. Woolford, and B. Crowder, (2011), "Intermediate Depth Drilling and Geophysical Logging Results at Superstition Mountain, Naval Air Facility El Centro, California", GRC Transactions, **35**.
- Tompson, A. F. B, Z. Demir, J. Moran, D. Mason, J. Wagoner, S. Kollet, K. Mansoor, and P. McKereghan (2008), Groundwater Availability Within the Salton Sea Basin: Final Report, Lawrence Livermore National Laboratory, Livermore, CA (LLNL-TR-400426).